



Synthesis and Characterization of Ni and Cu Doped ZnO Nanoparticles

Avneesh Kumar¹

¹Department of Physics, SVGC Ghumarwin, (H.P), INDIA

Abstract

In this article, exceptionally increase in production of nickel & copper doped zinc oxide nanostructures is reported. The ZnO nanostructures are synthesized with 10% of Ni & Cu doping adopting a Sol-gel method. Further the structural & Crystallite size studies were performed by utilizing X-ray diffraction. The identification of wurtzite phase and determination of lattice parameters of Ni & Cu doped ZnO nanocrystallites is ascertained. X-ray diffraction (XRD) results indicates that the crystallite size is in 23-39nm range, lattice parameters are $a=0.32\text{nm}$ and $c=0.52\text{nm}$ respectively for wurtzite structure of ZnO.

Keywords: nanoparticles, Precursor, zinc oxide, Sol-gel, XRD

1. Introduction

Valued for ZnO ultra violet absorbance, wide chemistry, piezoelectricity and luminescence at high temperatures, ZnO has penetrated far into industry, and is one of the critical buildings in today modern society.¹ ZnO is indeed a key element in many industrial manufacturing processes including paints, cosmetics, pharmaceuticals, plastic, batteries, electrical equipment, rubber, soap, textile, floor covering etc. with improvement in growth technology of ZnO nanostructures, single crystal and nanoparticles, ZnO devices will become increasing functional in the near future.² Metal oxide nanoparticles were extensively investigated due to their applications in the field of spintronics,³ photoelectronic,⁴ sensor,⁵ lasing devices⁶ and light emitting diodes,⁷ etc. The properties of these nano materials incredibly altered due to quantum confinement and enhanced surface to volume ratio.⁸ ZnO is a multifunctional material.⁹ The piezo- electric and pyroelectric properties of ZnO mean that it can be used as a sensor, converter, energy generator and photo catalyst in hydrogen production.¹⁰⁻²⁵ The physical and chemical properties of ZnO nano materials can be easily tailored as per the demand of device fabrication

1.1 Properties

ZnO is a relatively very soft material with approximate hardness just 4.5. Its elastic constants are relatively smaller than those of other III-V semiconductors, e.g. GaN. The high heat capacity and high heat conductivity, low values of thermal expansion and high melting points are 11 some of the characteristics of ZnO. Among the semiconductors bonded tetrahedrally, ZnO has the highest piezoelectric tensor. This makes it an important material for many piezoelectric applications, which require a high degree of electromechanical coupling among them. Piezoelectricity of ZnO has been extensively studied for various applications in force sensing, acoustic wave resonator, acousto-optic modulator, etc.¹¹

ZnO has a quite large band gap of 3.3eV at room temperature and 60meV excitation energy,¹² The advantages of a large band gap include higher values of breakdown voltages, sustaining large electric fields, high-temperature and high-power operations. ZnO has n-type character, in the absence of doping. Non-stoichiometry is usually the

origin of n-type character. Due to defects such as oxygen vacancies and zinc interstitials, P-type and n-type ZnO nano wires can serve as p-n junction diodes and light emitting diodes. Zinc oxide is generally transparent to visible light but strongly absorbs ultra violet light below 365.5nm many papers show its optical properties. The absorption in ZnO is stronger than other white pigments. In the region of visible wavelengths, regular zinc oxide appears white, but, rutilite and anatase titanium dioxide have a higher refractive index and thus has a superior opacity.¹³

The band gap energy (between valence and conducting bands) is 3.2eV. Under ultra violet light zinc oxide is photoconductive. The combination of optical and semiconductor properties of doped Zinc oxide make a contender for new generations of devices. Absorption of solar radiation in photovoltaic cells is much higher in materials composed of nanoparticles than it is in thin films of continuous sheets of material it means that they increase the efficiency, the smaller the particles, the greater the solar absorption.¹⁴

2. Experimental work

Doped Zinc oxide nanostructure was synthesized by using sol-gel method. To prepare a sol, precursor 0.2M of zinc acetate Dihydrate, .02M Nickel acetate (i.e. 10% Doping), reducing agent 0.2 M of sodium hydroxide were weighed using a weighing balance. Then 50ml of distilled water was measured by measuring cylinder for each sample. After that, all the weighing samples were dissolved separately in 50ml of distilled water. All the solutions were stirred with constant stirring for about 30 minutes. After well mixed, .02M Nickel acetate solution was poured to the solution containing zinc acetate with constant stirring by magnetic stirrer for about 30 minutes. Then 0.2 M of sodium hydroxide solution as reducing agent was poured to the solution containing zinc acetate & Nickel acetate with constant stirring by magnetic stirrer for about 1 hour. Then burette was filled with 100ml of PVA (Poly vinyl alcohol) and titrated dropwise to the solution containing reducing agent, zinc acetate and Nickel acetate. After the constant stirring, precipitates were formed. Dried precipitate was calcined at about 700°C for 24 hours in muffle furnace. So, we have produced Ni Doped ZnO nanoparticles. Similarly, Cu doped ZnO nanoparticles were prepared.

3. Result and Discussion

X-ray diffraction study confirms that the synthesized material was ZnO with wurtzite phase and the entire diffraction peaks are in agreement with the data available. The X-ray diffraction data were recorded by using Cu K α radiation ($\lambda=1.5406\text{\AA}$). The average grain size was calculated with the help of Scherrer equation using the FWHM of all peaks. Most importantly, all of the XRD peaks were attributed to ZnO and no other undesired peaks were observed due to secondary phases or impurity phases within the detection limit of the X-ray diffractometer.¹⁷

Scherrer equation is

$$D = 0.89\lambda / (\beta \cos\theta)$$

Where D is the grain size, λ is the wavelength of x-ray radiation, β is the full width at the half maximum (FWHM) of the ZnO and θ is the diffraction angle.

3.1 Based on Ni doped ZnO

Based on the experimental work that has been done, there are series of chemical reaction that takes place. The complete reaction is the transformation of Ni doped zinc acetate solution into Ni doped zinc oxide nanoparticles.

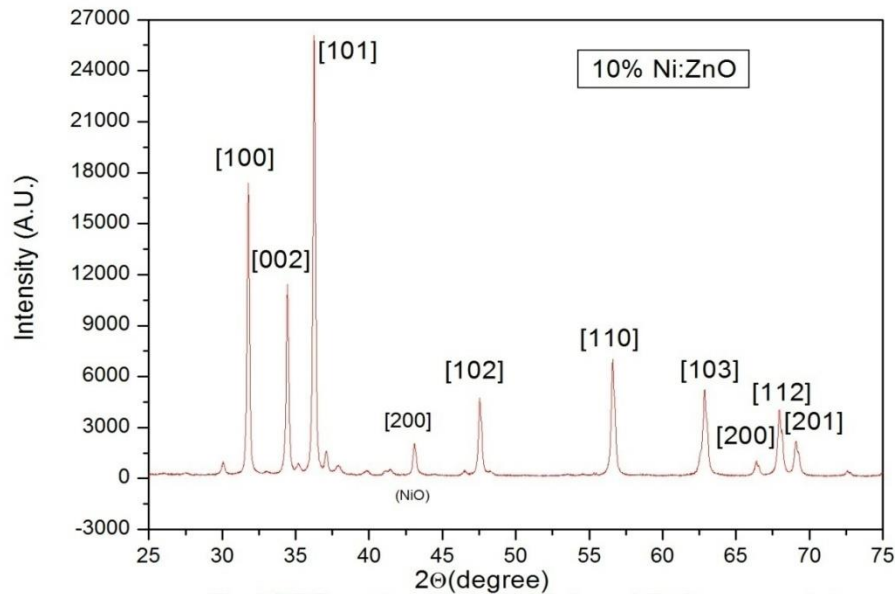


Fig.1 XRD pattern for 10% Ni doped ZnO nanoparticle

Table1: Crystallite Size(D): 10% Ni Doped ZnO NPs

Angle ($2\theta^\circ$)	θ°	θ (Radian)	$\text{Cos}(\theta)$	β°	β (Radian)	D (nm)	hkl	Average Size(D)(nm)
31.77	15.9	0.27725	0.962	0.21	0.003672	38.804	[100]	31.24
34.43	17.2	0.30046	0.955	0.211	0.003676	39.0299	[002]	
36.26	18.1	0.31643	0.95	0.21	0.003662	39.3823	[101]	
47.56	23.8	0.41504	0.915	0.262	0.004581	32.6953	[102]	
56.62	28.3	0.4941	0.88	0.312	0.005453	28.5471	[110]	
62.88	31.4	0.54873	0.853	0.386	0.006732	23.8619	[103]	
66.41	33.2	0.57954	0.837	0.355	0.006195	26.4438	[200]	
67.99	34	0.59332	0.829	0.358	0.006243	26.4805	[112]	
69.12	34.6	0.60319	0.824	0.367	0.006414	25.9496	[201]	

Table1. Indicate the average size of Ni doped ZnO nanoparticles is 31.24nm. In Fig.1, at 10% doping, we are getting, the NiO (200) XRD peak. This is due to the fact that doping of Ni is not completely substituted inside ZnO lattice and therefore, NiO phase is obtained besides ZnNiO phase. On the basis of x-ray diffraction, we infer that Ni doping in ZnO is responsible for transformation of nanoparticles to nanostructure (nanorods). The excess of Ni doping essentially drives the anisotropic growth of ZnNiO nanostructure and hence, nanorods formation takes place.

3.2 Based on Cu doped ZnO

Here the complete reaction is the transformation of Cu doped zinc acetate solution into Cu doped zinc oxide nanoparticle

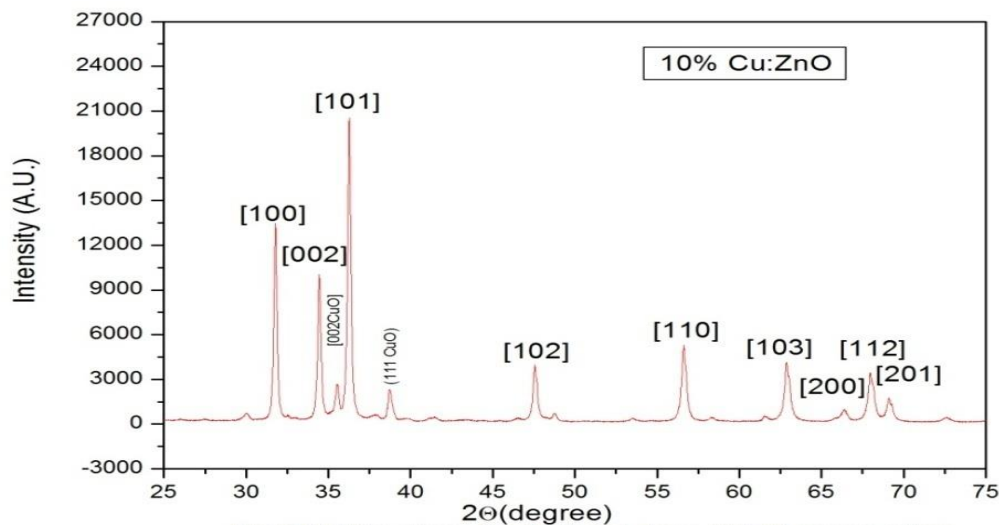


Fig.2 XRD pattern for 10% Cu doped ZnO nanoparticle

Table2: Crystallite Size(D): 10% Cu Doped ZnO NPs

Table2. Indicate the average size of Cu doped ZnO nanoparticles is 28.21nm. In Fig.2, at 10% doping, we are getting, the CuO (002) & (111) XRD peaks. This is due to the fact that doping of Cu is not completely substituted inside ZnO lattice and therefore, CuO phase is obtained besides ZnCuO phase. But overall, there is

Angle (2θ°)	θ°	θ (Radian)	Cos(θ)	β°	β (Radian)	βCos(θ)	D (nm)	hkl
31.77	15.89	0.27725	0.962	0.23	0.00404148	0.003887	35.26	[100]
34.44	17.22	0.30055	0.955	0.23	0.0040647	0.003882	35.3	[002]
36.27	18.14	0.31652	0.95	0.24	0.00418233	0.003975	34.48	[101]
47.57	23.79	0.41513	0.915	0.29	0.00509898	0.004666	29.37	[102]
56.63	28.32	0.49419	0.88	0.35	0.00613815	0.005404	25.36	[110]
62.91	31.46	0.54899	0.853	0.39	0.00680574	0.005806	23.61	[103]
66.37	33.19	0.57919	0.837	0.41	0.00708883	0.005933	23.1	[200]
68.01	34.01	0.5935	0.829	0.41	0.00706911	0.00586	23.39	[112]
69.13	34.57	0.60327	0.823	0.4	0.00692878	0.005706	24.02	[201]

Average size(D)=28.21nm

exceptionally increase in the production of nanostructure.

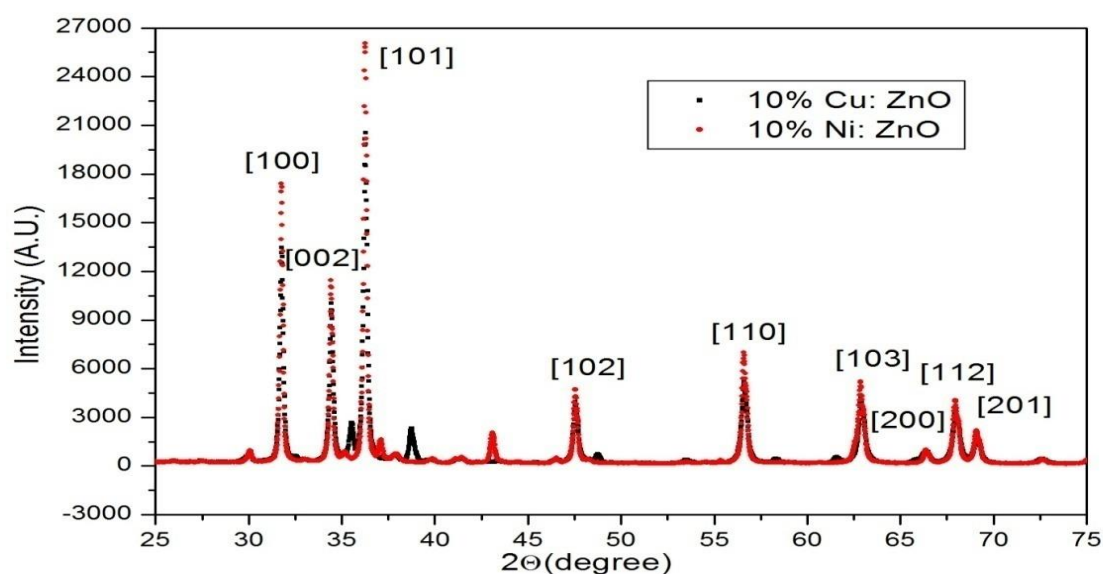


Fig.3 XRD pattern for 10% Cu&Ni doped ZnO nanoparticles

Fig3. Provides the comparative study of Ni & Cu doped ZnO nanoparticles.

4. Conclusion

The exceptionally increase in nickel & copper doped ZnO nanostructures can be summarized as follows. At 10% doping of Ni & Cu into ZnO, the Zn-O-Ni or Zn-O-Cu linkages become prominent without any change in phase and size of nanoparticles. Ni or Cu gives rise to weakening of Zn-O bonding and development of Ni-O or Cu-O interactions and Zn-O-Ni or Zn-O-Cu linkages and subsequently favours anisotropic growth in ZnNiO or ZnCuO nanostructures. As a consequence, exceptionally increase of nanostructures takes place. Also, X-ray diffraction (XRD) results indicates that the crystallite size is in 23-39nm range, lattice parameters are $a=0.32\text{nm}$ and $c=0.52\text{nm}$ respectively for wurtzite structure of ZnO.

References

1. Eric Drexler K. *Engines of Creation: The Coming Era of Nanotechnology*. Doubleday; 1986. p. 1–10.
2. European Commission. The 7th frame program.
3. Meron T, Markovich G. Ferromagnetism in Colloidal Mn^{2+} -Doped ZnO Nanocrystals. *J Phys Chem B*. 2005;109(43):20232–20236.
4. Liang S, Sheng H, Liu Y, et al. ZnO Schottky ultraviolet photodetectors. *Journal of Crystal Growth*. 2001;225(2-4):110–113.
5. Shishiyanu ST, Shishiyanu TS, Lupan OI. Sensing characteristics of tin-doped ZnO thin films as NO_2 gas sensor. *Sensors and Actuators B*. 2005;107:379–386.
6. Huang MH, Mao S, Feick H, et al. Room-temperature ultraviolet nanowire nanolasers. *Science*. 2001;292(5523):1897–1899.
7. Saito N, Haneda H, Sekiguchi T, et al. Low-temperature fabrication of light-emitting zinc oxide micropatterns using self-assembled mono-layers. *Advanced Materials*. 2002;14(6):418–421.
8. Ma Y, Ricciuti C, Miller T, et al. Enhanced catalytic combustion using sub-micrometer and nano-size platinum particles. *Energy Fuels*. 2008;22(6):3695–3700.
9. Segets D, Gradl J, Taylor RK, et al. Analysis of optical absorbance spectra for the determination of ZnO nanoparticle size distribution, solubility, and surface energy. *ACS Nano*. 2009;3(7):1703–1710.
10. Chaari M, Matoussi A. Electrical conduction and dielectric studies of ZnO pellets. *Physica B: Physics of Condensed Matter*. 2012;407(17):3441–3447.
11. Corso AD, Posternak M, Resta R, et al. Ab initio study of piezoelectricity and spontaneous polarization in ZnO. *Physical Review B*. 1994;50(15):10715.

12. Wang ZL. Zinc oxide nanostructures: growth, properties and Applications. *Journal of Physics Condensed Matter*. 2004;16:R829–R858.
13. Becheri A, Durr, M, Nostro PL, et al. Synthesis and characterization of zinc oxide nanoparticles: application to textiles as UV-absorbers. *Journal of Nanoparticle Research*. 2008;10(4):679–689.
14. Schaller RD, Klimov VI. High efficiency carrier multiplication in PbSe nanocrystals: implications for solar energy conversion. *Physical Review Letters*. 2004;92:186601.
15. Liz-Marzan LM. Tailoring surface plasmons through the morphology and assembly of metal nanoparticles. *Langmuir*. 2006;22(1):32–41.
16. Rodrigues P, Caballero J, Villegas AC, et al. Controlled precipitation methods: formation mechanism of ZnO nanoparticles. *Journal of the European Ceramic Society*. 2001;21(7):925–930.
17. Bragg WH. *Phil Mag*. 1912;23:136
18. R. P. Wang, G. Xu, P. Jin, *Phys. Rev. B* 69, 113303 (2004).
19. B. Cheng, Y. Xiao, G. Wu, L. Zhang, *Appl. Phys. Lett.* 84, 416 (2004).
20. L. W. Yang, X. L. Wu, G. S. Huang, T. Qiu, Y. M. Yang, *J. Appl. Phys.* 97, 014308 (2005).
21. K. A. Alim, V. A. Fonoberov, A. A. Balandin, *Appl. Phys. Lett.* 86, 053103 (2005).
22. K. Uma, S. Ananthakumar, R. V. Mangalaraja, K. P. O. Mahesh, T. Soga, T. Jimbo, *J. Sol-Gel Sci. Techn.* 49 (1), 1 (2009).
23. S. K. Panda, C. Jacob, *Bull. Mater. Sci.* 32 (5), 493 (2009).
24. N. M. Ulmane, A. Kuzmin, I. Steins, J. Grabis, I. Sildos, M. Pärs, *J. Phys.: Conf. Ser.* 93, 012039 (2007).
25. T. C. Damen, S. P. S. Porto, B. Tell, *Phys. Rev.* 142 (2), 570 (1966).

